Journal of Applied Polymer Science

Climate-friendly polyurethane blowing agent based on a carbon dioxide adduct from palmitic acid grafted polyethyleneimine

Yuanzhu Long, Fuhua Sun, Chao Liu, Dong Huang, Xingyi Xie
College of Polymer Science and Engineering, Sichuan University, Chengdu, Sichuan 610065, China
Correspondence to: X. Xie (E-mail: xiexingyi@263.net)

ABSTRACT: To explore a new blowing agent for polyurethanes (PUs), palmitic acid was grafted onto a branched polyethyleneimine (bPEI; weight-average molecular weight = 25,000 Da) via *N,N′*-carbonyldiimidazole condensation to form a hydrophobically modified bPEI [palmitic acid grafted branched polyethyleneimine (C_{16}–bPEI)] with a grafting rate of 12%. A CO_2 adduct of C_{16}–bPEI, which trapped 16.8% CO_2 in it, was synthesized from C_{16}–bPEI. The long alkyl chain grafting improved the dispersibility of the CO_2 adduct in the PU raw materials and favored a homogeneous release of CO_2 to blow PUs during the exothermic foaming process. The preliminary results show that the foams possessed a density of 72.0 kg/m^3 and a compressive strength of 246 kPa; this matched the required values of foams for the thermal insulation of underground steel pipes. This new blowing agent emitted nothing but CO_2 to the atmosphere, so it will not promote ozone depletion and will avoid global warming problems that are associated with traditional blowing agents such as chlorofluorocarbons and hydrochloroflourocarbons. © 2016 Wiley Periodicals, Inc. J. Appl. Polym. Sci. **2016**, *133*, 43874.

KEYWORDS: foams; polyurethanes; synthesis and processing

Received 20 January 2016; accepted 25 April 2016
DOI: 10.1002/app.43874

INTRODUCTION

The total consumption of polyurethane (PU) foams in China reached 3.4 million tons in 2014 with an annual growth rate of 7%.[1] Their manufacturing requires large amounts of blowing agents; these are climate-changing substances that are regulated by Montreal and Tokyo Protocols. Traditional chlorofluorocarbons have been banned because of the severe destruction that they cause to the stratospheric ozone layer.[2–6] Currently used hydrochloroflourocarbons and hydrofluorocarbons are greenhouse gasses, whose global warming potential is hundreds of times higher than that of CO_2.[3–6] Water has been used as a chemical blowing agent; it generates CO_2 *in situ* by reaction with isocyanate raw materials of PU.[7,8] This foaming reaction is highly exothermic; this possibly causes heartburn and even the self-ignition of the foams if too much water is used. Another problem associated with water-blown PUs is that the foams are usually brittle because of abundant urea linkages in the PU chains. Foaming with liquid CO_2 has been introduced[9–12]; however, it requires a complicated storage and metering system for CO_2. Volatile hydrocarbons such as cyclopentane belong to climate-friendly blowing agents,[13–15] although they are highly flammable. Therefore, the exploration of a safe, climate- and user-friendly blowing agent is very urgent in the PU foam industry.

Because of the high density of amino groups in their molecular structure, polyethyleneimines (PEIs) are effective at absorbing CO_2, and they have been widely investigated to capture CO_2 as a means to relieve global warming.[16–21] In a recent publication,[22] we proved that CO_2 adducts from PEIs can be used as climate-friendly blowing agents for PUs. In that study, a branched polyethyleneimine (bPEI) was grafted with α-glycidyl ether-ω-butyl poly(propylene glycol) (PPG) with a molecular weight of 392 Da. The hydrophobic PPG side chains made the resulting bPEI and its CO_2 adduct dispersible in PU raw materials. This dispersibility is a prerequisite for a steady foaming process. A CO_2-releasing blowing agent with 13.8% CO_2 in it was obtained from the PPG-grafted bPEI.

In this study, we attempted to graft bPEI with a long alkyl side chain from palmitic acid to test the feasibility of the resulting CO_2 adduct as a new blowing agent for PUs. This blowing agent was compatible with PU raw materials and could trap more CO_2 than previous PPG-grafted bPEI (16.8 vs. 13.8%) because of the shorter side chain in the former. We believe this basic study was essential in optimizing the chemical structure and improving the foaming efficiency of PEI-based CO_2-releasing blowing agents.

Additional Supporting Information may be found in the online version of this article.

© 2016 Wiley Periodicals, Inc.

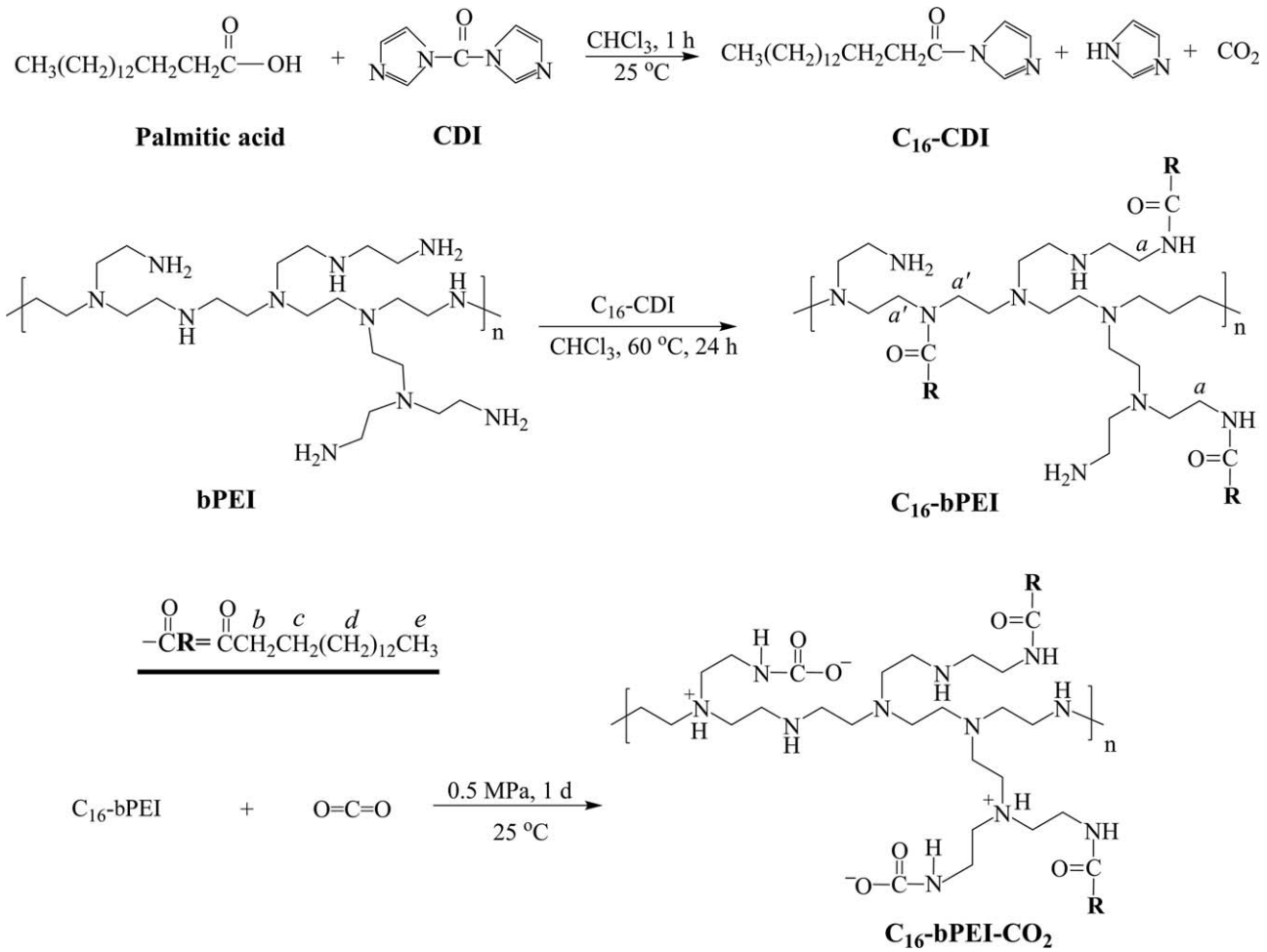

Figure 1. Synthesis of C_{16}–bPEI and C_{16}–bPEI–CO_2. Some protons are labeled for the assignment of the ^{1}H-NMR spectra in Figure 2(A).

EXPERIMENTAL

Synthesis of Palmitic Acid Grafted Branched Polyethyleneimine (C_{16}–bPEI)

In a 250-mL, three-necked, round-bottomed flask, 3.578 g (13.95 mmol) of palmitic acid and 2.262 g (13.95 mmol) of *N,N′*-carbonyldiimidazole (CDI; both from Aladdin, China) were dissolved in 50 mL of chloroform and stirred for 1 h at room temperature. Then, 5 g of bPEI (number-average molecular weight = 25,000 Da; Sigma-Aldrich, United States) in 150 mL of chloroform was added, and the temperature was increased to 60 °C. Note that the amino group in PEI was 116 mmol, and the theoretical grafting rate was set at 12%. After 1 day of reaction, the reaction mixture was extracted with 150 mL of saturated NaCl solution eight times. Finally, the organic phase was dried with Na_2SO_4 overnight, and the solvent was removed by rotational evaporation to obtain C_{16}–bPEI (see Figure 1).

Synthesis of CO_2 Adducts of bPEI (bPEI–CO_2) and C_{16}–bPEI (C_{16}–bPEI–CO_2)

To synthesize bPEI–CO_2 as a control, 3 g of bPEI in 6 mL of ethanol was purged with CO_2 gas for 10 min, and a white precipitate emerged. After another 30 min of purging, the precipitate was transferred onto a watch glass and dried at 40 °C for 96 h. The dried product was put into a steel container to further absorb CO_2 at 1.5 atm for 8 h. Then, it was ground into powder and saturated with CO_2 in the same container for at least 1 day.

C_{16}–bPEI absorbed CO_2 much faster than the original bPEI. Thus, C_{16}–bPEI as a white solid was cut into pieces and exposed to CO_2 at 0.5 MPa for 4 h. Then it was ground into powder and saturated with CO_2 for another 20 h to obtain C_{16}–bPEI–CO_2 (Figure 1).

Preparation of the PU Foams

All of the raw materials (Table I) for the PU foams were from Advanced Polymers Co., Ltd. (Chengdu, Sichuan, China). The ingredients, which consisted of the white component (blank and formulations I–III; Table I), were mixed in a plastic cup through stirring at 1000 rpm for 30 s. The black component (Table I) was then added, and the mixture was stirred at 1400 rpm for another 15 s. The beginning of this stirring was set as 0 s. The mixture turned white and foamed freely until solidification. The whitening time, the maximum foam-height time, and the tack-free time were recorded. Another set of foams were prepared in the same way after the white component was aged (formulations I–III; Table I) for 3 days at room temperature. All of the prepared foams were aged at room temperature for at least 4 days before any characterization was undertaken. Note that foams from the blank formulation (without an external blowing

Table I. Formulations of the PU Foams

Raw material	Description	Formulation (g)			
		Blank	I	II	III
White component					
Polyether 4110	Four-arm poly(propylene glycol); OH value, 430 mg of KOH/g	8.50	8.50	8.50	8.50
Silicone L-3102	Foam stabilizer	0.16	0.16	0.26	0.26
Stannous octoate (T-9)	Catalyst	0.02	0.02	0.02	0.02
Triethylenediamine (A-33)	Catalyst, 33 wt % in ethylene glycol	0.20	0.20	0.04	0.04
Tris(1-chloro-2-propyl) phosphate	Diluent and flame retardant	7.15	7.15	7.30	7.30
Propylene glycol	Chain extender	0	0	0.06	0.06
Diethanol amine	Crosslinking agent	0	0	0.20	0.20
H_2O	Blowing agent	—	—	—	0.22
bPEI-CO_2 or C_{16}-bPEI-CO_2	Blowing agent	—	0.50	3.00	—
Black component: PMDI[a]	—NCO content, 31 wt %	9.60	9.60	15.0	15.0
Isocyanate index[b]		1.01	1.01	1.37	1.08

[a] Polymeric 4,4′-diphenylmethane diisocyanate.
[b] Isocyanate indices were calculated under the assumption that bPEI-CO_2 and C_{16}-bPEI-CO_2 did not participate in the polymerization of PUs. Also, the water impurity (0.04 g) in polyether 4110 and the ethylene glycol in A-33 were included for all calculations.

agent) and formulation III (with external water as the blowing agent) served as controls.

Characterization

To test the dispersibility of the blowing agents, the thoroughly mixed white component (formulation I; Table I) with 0.5 g of C_{16}–bPEI–CO_2 or bPEI–CO_2 was aged for 3 days at room temperature. The macroscopic photographs were recorded with a digital camera. Each white component was homogenized by shaking before morphological observation under an Olympus BX 43 light microscope (Olympus, Japan). The change in the chemical structure after each step of synthesis was monitored by Fourier transform infrared spectroscopy (Nicolet 560 IR spectrometer, Nicolet Instruments) and ^{1}H-NMR spectroscopy (Varian 400-MHz NMR spectrometer, Varian, Inc.). To measure the CO_2 content of each blowing agent, thermogravimetry (TG) analysis was performed on a TG 209F1 apparatus (Netzsch Instruments, Germany) at 10 °C/min under a nitrogen flow of 100 mL/min. The enthalpy change (ΔH) due to CO_2 release was measured by differential scanning calorimetry (DSC) on a PE DSC-2C instrument (PerkinElmer) with the same operation conditions used for TG analysis. The density of the PU foams was obtained by the accurate measurement of the volume and weight of each specimen (ca. $30 \times 30 \times 20$ mm^3 in size with a foam rise direction parallel to the 20-mm edges, $n = 10$). The same specimens ($n = 5$) were compressed at the foam rise direction on an Instron 5507 universal testing machine (Instron Corp.) at 3 mm/min to obtain the mechanical properties. The cellular morphology was examined under a JSM-9600 scanning electron microscope (JEOL, Japan).

RESULTS AND DISCUSSION

Chemical Structures of C_{16}–bPEI, C_{16}–bPEI–CO_2, and bPEI–CO_2

As shown in Figure 2(A), bPEI displayed proton signals of CH_2—N at 2.3–2.9 ppm and amino groups (—NH— and —NH_2) at about 1.9 ppm. C_{16}–bPEI retained the methylene signals of the bPEI backbone and showed a series of new signals: overlapped *a* and *a*′ ranging between 3.15 and 3.55 ppm and individual signals *b*–*e* centered at 2.15, 1.59, 1.24, and 0.86 ppm, respectively. The signals *a* and *a*′ were due to the CH_2 groups adjacent to the side chains that attached to the primary and secondary amino sites in the original bPEI backbone, respectively (Figure 1); the ratio of such primary to secondary amino sites was 2:3, as calculated from the integration ratio of signal $a + a'$ to signal *c* (3.21:2). The chemical shifts and peak areas of signals *b*–*e* matched the structure of the *n*-pentadecylcarbonyl side chain [Figures 1 and 2(A)]. We noted that the signal of α-CH_2 from palmitic acid was at about 2.3 ppm; this was absent in the NMR spectrum of C_{16}–bPEI; this suggested its high purity. In the C_{16}–bPEI spectrum, the N—H signal overlapped with the CH_2—N signals. The former was shifted downfield to about 3.3 ppm by the addition of CD_3OD. Thus, the relative peak area of the backbone CH_2—N signals and the side-chain signal *c* [31.01:2.00; Figure 2(A)] was used to calculate the grafting rate, which was 12.1% [Table II and Figure S1 and eq. (S1) in the Supporting Information]. This was consistent with the theoretical value of 12% calculated from the feed ratio of the raw materials. The side-chain content and valid PEI content (Table II) were calculated on the basis of the measured grafting rate. The valid PEI linkages could react with CO_2, whereas those grafted with the side chains were incapable of absorbing CO_2.

As shown in Figure 2(B), the Fourier transform infrared spectrum of bPEI showed typical amine adsorptions (ν_{N-H} at 3360 cm^{-1} and δ_{N-H} at 1652, 1580, and 1467 cm^{-1}) and aliphatic CH_2 adsorptions (ν_{C-H} at 2970 and 2834 cm^{-1}). Apart from these bands, new peaks related to $\nu_{C=O}$ (1642 cm^{-1} in H-bonded amide) and δ_{CH3} (1363 cm^{-1} in the *n*-pentadecylcarbonyl side chain) emerged in the C_{16}–bPEI spectrum (as indicated by asterisks); this further confirmed the success of the grafting reaction.

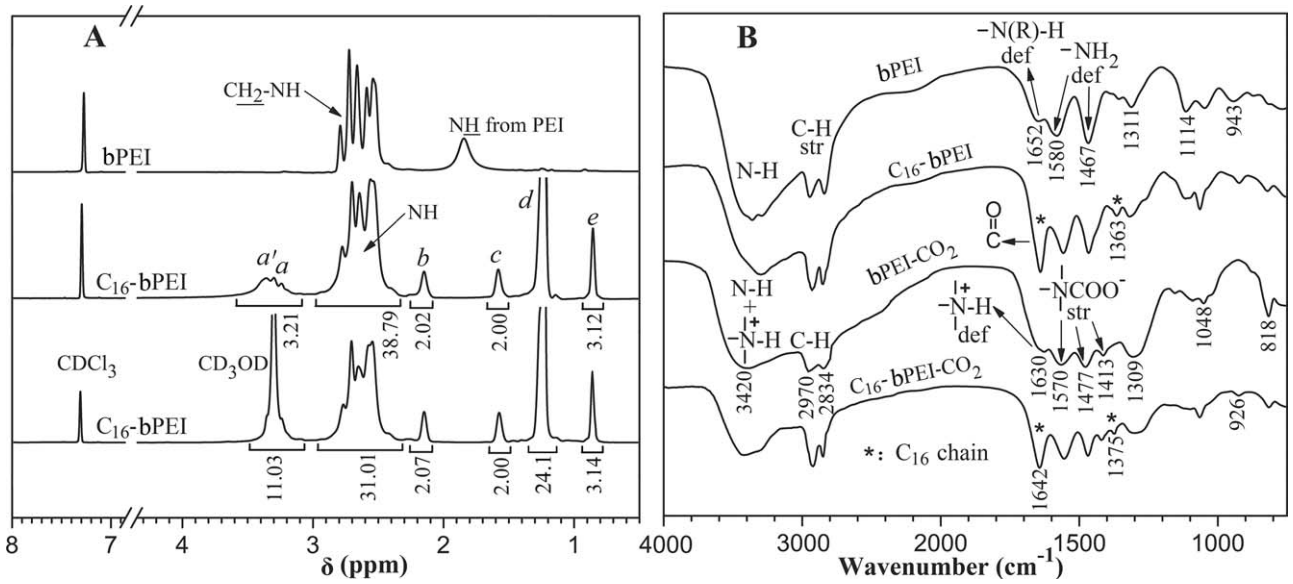

Figure 2. Spectroscopic analyses of bPEI, C_{16}–bPEI, and their CO_2 adducts: (A) the addition of CD_3OD shifted the —NH— signal downfield in C_{16}–bPEI. The relative peak area of CH_2—N to H_c (31.01:2.00) was used to calculate the grafting rate, and (B) C_{16}–bPEI–CO_2 displayed typical IR adsorptions from carbamate anions and *n*-pentadecylcarbonyl side chains (as indicated by asterisks).

The CO_2 adduction formed carbamate anions and alkylammonium cations in both bPEI–CO_2 and C_{16}–bPEI–CO_2 (Figure 1). As a result, a group of strong IR bands at 1630, 1570, 1477, and 1413 cm^{-1} [Figure 2(B)] emerged in bPEI–CO_2; these could be assigned to δ_{N-H} in ammonium,[23] $\nu_{C=O}$ in carbamate,[24] and the asymmetrical and symmetrical skeletal stretching of carbamate anions,[22] respectively. The ν_{N-H} adsorptions in both alkylammonium (from 2200 to 3200 cm^{-1}) and —$NHCOO^-$ (3420 cm^{-1}) groups fused together and formed a very broad peak that spanned from 2200 to 3700 cm^{-1} and covered the aliphatic ν_{C-H} adsorptions. C_{16}–bPEI–CO_2 inherited the typical adsorptions of bPEI–CO_2 and displayed new adsorptions from the *n*-pentadecylcarbonyl side chains [also indicated by asterisks, Figure 2(B)].

Both bPEI–CO_2 and C_{16}–bPEI–CO_2 demonstrated an obvious weight loss upon heating, whereas the control sample C_{16}–bPEI maintained its original weight well before 200 °C (Figure 3). Accordingly, both CO_2 adducts displayed a broad and irregular endothermic peak that spanned the same temperature range as the corresponding weight loss process. No ΔH was measured in C_{16}–bPEI. It was reasonable that both the weight loss and endothermic process were due to the release of CO_2 from the CO_2 adducts. The measured CO_2 contents and ΔH values are summarized in Table II. The theoretical CO_2 contents were calculated (see Figure S2 in the Supporting Information) on the basis of the fact that two amino groups absorbed one CO_2 molecule.[25] On the basis of the data in Table II, we concluded that bPEI–CO_2 was saturated with CO_2, whereas C_{16}–bPEI–CO_2 did not reach saturation yet.

The upper limit of the CO_2 release temperature range in bPEI–CO_2 was higher than that in C_{16}–bPEI–CO_2 (182 vs. 147 °C, dashed line in Figure 3); this suggested that grafting with hydrophobic side chains facilitated the release of CO_2. This was similar to our previous observation in PPG-grafted bPEI.[22] Because of the steric hindrance, palmitic acid molecules preferably grafted onto primary amines rather than secondary amines of

Table II. Important Parameters for C_{16}–bPEI, bPEI–CO_2, and C_{16}–bPEI–CO_2

Material	Parameter	Theoretical	Measured	Testing method
C_{16}-bPEI	Grafting rate (%)	12.0	12.1	^{1}H-NMR
	Side-chain ($C_{15}H_{31}CO$—) content (wt %)		40.3	
	Valid PEI content (wt %)		52.6	
bPEI-CO_2	CO_2 content (%)	33.8	34.1	TG
	Measured ΔH (J/g)		365	DSC
C_{16}-bPEI-CO_2	CO_2 content (%)	21.2	16.8	TG
	Measured ΔH (J/g)		154	DSC
	Normalized ΔH (J/g)		254	

The calculation of these parameters is shown in the Supporting Information.

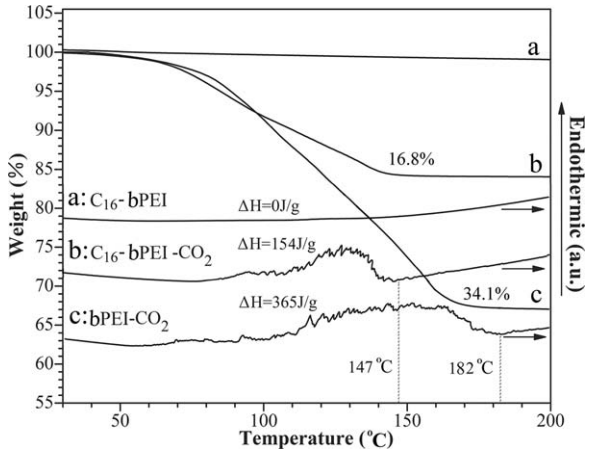

Figure 3. TG and DSC curves of the CO_2 adducts of bPEI and C_{16}–bPEI. The original C_{16}–bPEI served as a control.

bPEI; this resulted in fewer primary amines in C_{16}–bPEI than in bPEI. Consequently, secondary amine derived carbamate anions (>NCOO$^-$) predominated in C_{16}–bPEI–CO_2, whereas primary amine derived ones (—NHCOO$^-$) remained at a higher content in bPEI–CO_2. The latter anions can form intermolecular hydrogen bonds; this makes them more difficult to decompose than >NCOO$^-$ anions. This explained well the higher CO_2 release temperatures in bPEI–CO_2 than in C_{16}–bPEI–CO_2. For the same reason, a higher ΔH value should have been measured in bPEI–CO_2 than in C_{16}–bPEI–CO_2; in fact, the values were 365 and 154 J/g (Table II), respectively. Taking into consideration the fact that the side-chain-attached PEI repeating units in C_{16}–bPEI could not absorb CO_2, the weight of these units was excluded in the calculation of the normalized ΔH of C_{16}–bPEI–CO_2 [see eq. (S2) in the Supporting Information]. This normalized value (254 J/g) was still lower than the ΔH value of bPEI–CO_2 (Table II).

Dispersibility of C_{16}–bPEI–CO_2 with the PU Raw Materials

Figure 4 shows the morphological change of the white component containing C_{16}–bPEI–CO_2 or bPEI–CO_2. Basically, the blank sample did not show any particles before or after aging. After three-day aging, the macroscopic photos demonstrated that bPEI–CO_2 precipitated from the white component (see arrow, Figure 4), whereas C_{16}–bPEI–CO_2 still dispersed very well. Microscopically, the bPEI–CO_2 white component displayed large particles throughout aging. The particles of C_{16}–bPEI–CO_2, on the other hand, were suspended well and gradually decreased in size with time, and some of them displayed a spherical micellelike morphology after aging. The hydrophobic alkyl chains from palmitic acid was effective in dispersing the CO_2 adduct into the white component.

PU Foaming with the New Blowing Agent

Table III presents the effect of different blowing agents on the PU foaming speed. The blank samples (without blowing agent) were blown by water in the raw materials and showed relatively low foaming speed. Overall, the foaming process was accelerated by the addition of bPEI–CO_2 or C_{16}–bPEI–CO_2. The whitening time was shortened because more bubbles were generated in the foaming system by the corresponding CO_2 adduct compared to the blank system. Meanwhile, the release of CO_2 gradually restored the polyamine structure of the the original bPEI or C_{16}–bPEI. The restored amino groups quickly reacted with the isocyanate groups in the growing PU chains or catalyzed the chain growth reaction of PU; this shortened both the foam rising time and the tack-free time. The long alkyl side chains in C_{16}–bPEI–CO_2 provided steric hindrance to the restored amino groups and thus inhibited their participation in the PU chain growth reaction to some extent; this lowered the foaming speed, compared with that of the bPEI–CO_2 foaming system. As for formulations I and II (Table I), more blowing agent and less catalyst [triethylenediamine (A-33)] were used in the latter,

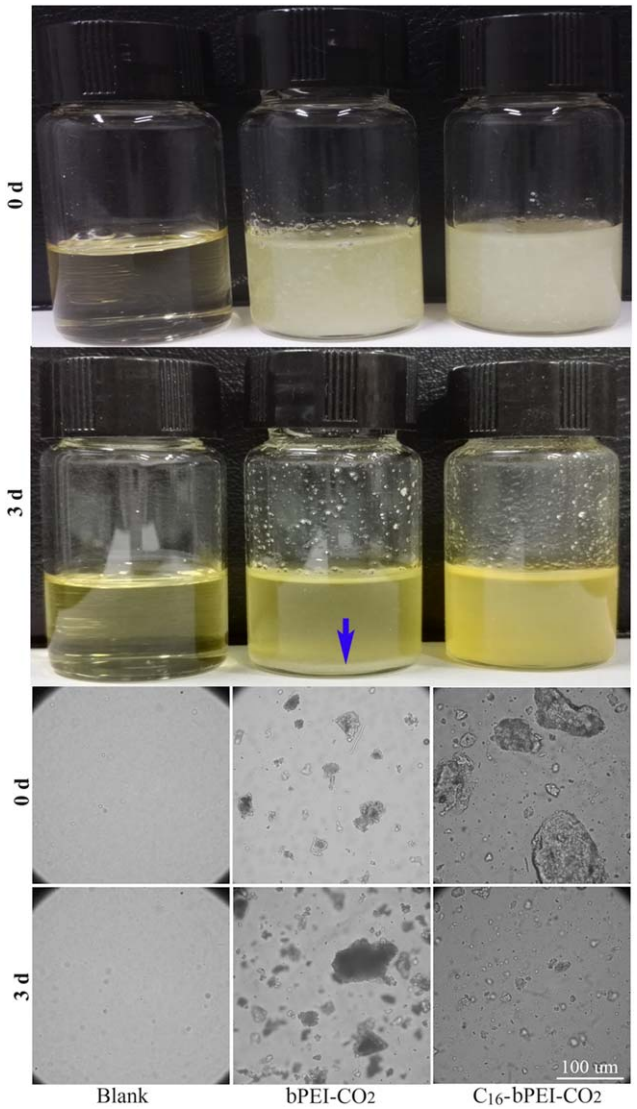

Figure 4. Morphological changes during the aging of the white component with 0.5 g of the blowing agent (formulation I in Table I). The blank sample served as a control. The arrowed line indicates the precipitate at the bottom. [Color figure can be viewed in the online issue, which is available at wileyonlinelibrary.com.]

Table III. Foaming Parameters of the Formulations Based on Various Blowing Agents

Blowing agent	Formulation	Whitening time (s)	Maximum foam-height time (s)	Tack-free time (s)	Maximum exotherm temperature (°C)
Blank		26	90	105	106
bPEI-CO_2	I	18	78	94	104
	II	44	195	325	102
C_{16}-bPEI-CO_2	I	23	84	99	102
	II	52	221	407	99
Water	III	46	205	373	119

whose overall polymerization speed was significantly lowered. This allowed more time for the release of CO_2 before the solidification of the foaming system of formulation II.

Table III further shows that the foaming speed in the water-blown system (formulation III) was faster than that in the C_{16}–bPEI–CO_2 blown system (formulation II), although the final densities of both foams were statistically identical [Figure 5(A)]. The maximum exotherm temperature of the water-blown system was much higher as well (119 vs. 99 °C). Both phenomena were not surprising because the reaction between water and

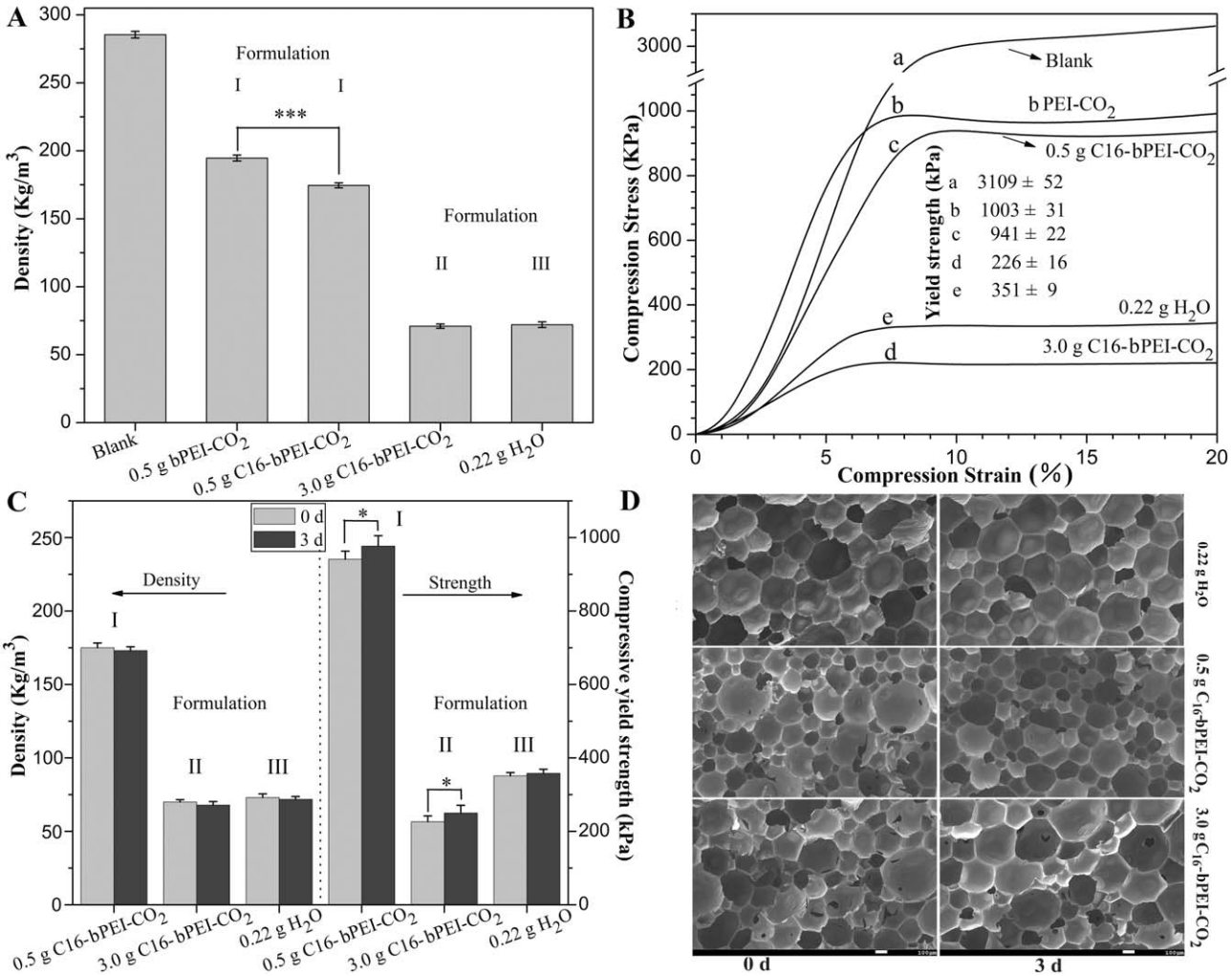

Figure 5. Effects of the blowing agent loading and white component aging on the PU foam morphology and properties: (A,B) increases in the C_{16}-bPEI–CO_2 loading decreased the density and compressive strength and (C,D) the aging of the white component containing C_{16}-bPEI–CO_2 for 3 days homogenized the pore size and increased the compressive strength, but the density was retained. Aging had no effects on the water-blown foams. The scale bar in panel D represents 100 μm. $^{***}p < 0.001$. $^{*}p < 0.05$ (Student t test).

isocyanates was highly exothermic, whereas CO_2 release from the CO_2 adducts was endothermic (Figure 3).

As shown in Figure 5(A), all of the foams blown by the CO_2 adduct possessed much lower densities than the blank foams; this further confirmed that CO_2 was released during the foaming process. With the same amount of blowing agent used (0.5 g, formulation I; Table I), the foams blown by C_{16}–bPEI–CO_2 displayed a lower density than those blown by bPEI–CO_2, although the latter trapped twice as much CO_2 as the former. This indicated that CO_2 was not fully released from bPEI–CO_2; this was most likely due to its higher CO_2 release temperatures (Figure 3) and its too fast foaming speed (Table III). The latter may cause the solidification of the foaming system before the complete release of CO_2. This was not the case in C_{16}–bPEI–CO_2. With the lower CO_2 release temperatures and slower foaming process, C_{16}–bPEI–CO_2 released CO_2 more completely. More significantly, C_{16}–bPEI–CO_2 was more dispersible in the raw materials of PU (Figure 4) with more nuclei to release CO_2 than bPEI–CO_2. Obviously, more but smaller bubbles formed in the foaming mixture containing C_{16}–bPEI–CO_2, and thus, they had a lower chance to break. All of these factors favored a reduction in the density of the C_{16}–bPEI–CO_2 blown foams.

With increasing C_{16}–bPEI–CO_2 amount from 0.5 to 3.0 g (i.e., from formulation I to formulation II; Table I), the foam density decreased to about 72.0 kg/m^3 [Figure 5(A)] with a compressive yield strength of 246 kPa [Figure 5(B)]. Both data matched the required values of thermal insulation foams for underground pipes (the acceptable density was in the range of 30–80 kg/m^3, and the compressive strength should have been higher than 100 kPa according to Chinese standard SY/T 0415). The compressive strength generally increased with increasing density [Figure 5(B)]. However, the foams made from the white component that were aged for 3 days at room temperature displayed a slight but significant increase in the mechanical strength without changes in the foam density [Figure 5(C)]. The aging improved the dispersibility of C_{16}–bPEI–CO_2 and resulted in more homogenized pore sizes in the PU foams [Figure 5(D)] and thus increased the mechanical strength. On the contrary, the same aging had no effects on the mechanical strength and morphology of the water-blown foams [Figure 5(C,D)]. These foams were stronger than the C_{16}–bPEI–CO_2 blown foams at almost the same density [Figure 5(A,B)]. This was because the greater number of urea linkages in the water-blown foams caused stronger intermolecular H bonding, compared with the C_{16}–bPEI–CO_2 blown analogues.

Overall, the hydrophobic modification of bPEI with palmitic acid was an effective method toward the development of climate-friendly CO_2-releasing blowing agents for PUs. The CO_2 content in the blowing agent of this study (16.8%) surpassed the reported value (13.8%) in a similar blowing agent from PPG-grafted PEI.[22] This was mainly because the molar mass of the side chains ($C_{15}H_{31}CO$—, 239.4 Da) in C_{16}–bPEI was much lower than that of previously used PPG side chains (392 Da); this resulted in relatively more PEI linkages that could absorb CO_2 in the former at the same grafting yield. Future work will optimize the side-chain length and grafting rate for better blowing agents.

CONCLUSIONS

The palmitic acid grafted PEI with a grafting rate of 12% could absorb CO_2 and then release CO_2 to blow PUs. The hydrophobic side chains improved the dispersibility of the resulting blowing agent in the PU raw materials and favored the preparation of PU foams with a uniform cell size and good mechanical properties. The current foams possessed density and mechanical strength values similar to those of foams for the thermal insulation of underground steel pipes. The long alkyl modification of PEI is a new method for preparing CO_2 adducts as climate-friendly blowing agents for PU foams.

ACKNOWLEDGMENTS

The authors greatly appreciate the financial support of the Natural Science Foundation of China (contract grant number 51173111).

REFERENCES

1. Zhu, C.; Lv, G. *Polyurethane Ind.* **2015**, *30*, 1.
2. Yin, L.; Lin, J. *Guangzhou Chem. Ind.* **2015**, *43*, 43.
3. Naik, V.; Jain, A. K.; Patten, K. O. D.; Wuebbles, J. *J. Geophys. Res.* **2000**, *105*, 6903.
4. Danny, H. L. D. *Build. Environ.* **2007**, *42*, 2860.
5. Kim, K. H.; Shon, Z. H.; Nguyen, H. T.; Jeon, E. C. *Atmos. Environ.* **2011**, *45*, 1369.
6. Grolier, J. E.; Randzio, S. L. *J. Chem. Thermodyn.* **2012**, *46*, 42.
7. Wada, H.; Fukuda, H. *J. Cell. Plast.* **2009**, *45*, 293.
8. Sonnenschein, M. F.; Wendt, B. L. *Polymer* **2013**, *54*, 2511.
9. Kim, C.; Youn, J. R. *Polym. Plast. Technol. Eng.* **2000**, *39*, 163.
10. Fieback, T.; Michaeli, W.; Latz, S.; Mondéjar, M. E. *Ind. Eng. Chem. Res.* **2011**, *50*, 7631.
11. Dai, C.; Zhang, C.; Huang, W.; Chang, C. L.; Lee, J. *Polym. Eng. Sci.* **2013**, *53*, 2360.
12. Hopmann, C.; Latz, S. *Polymer* **2015**, *56*, 29.
13. Bazzo, W.; Cappella, A.; Talbot, S. *J. Cell. Plast.* **1996**, *32*, 46.
14. Park, D. H.; Park, G. P.; Kim, S. H.; Kim, W. N. *Macromol. Res.* **2013**, *21*, 852.
15. Hossieny, N. J.; Barzegari, M. R.; Nofar, M.; Mahmood, S. H.; Park, C. B. *Polymer* **2014**, *55*, 651.
16. Xu, X.; Song, C.; Miller, B. G.; Scaroni, A. W. *Fuel Process. Technol.* **2005**, *86*, 1457.
17. Son, W. J.; Choi, J. S.; Ahn, W. S. *Microporous Mesoporous Mater.* **2008**, *113*, 31.
18. Le, M. U. T.; Lee, S. Y.; Park, S. J. *Int. J. Hydrogen Energy* **2014**, *39*, 12340.
19. Jung, H.; Jo, D. H.; Lee, C. H.; Chung, W.; Shin, D.; Kim, S. H. *Energy Fuel.* **2014**, *28*, 3994.

20. Liu, H.; Chen, Y.; Zhu, D.; Shen, Z.; Stiriba, S. E. *React. Funct. Polym.* **2007**, *67*, 383.

21. Sehaqui, H.; Galvez, M. E.; Becatinni, V.; Cheng, N. Y.; Steinfeld, A.; Zimmermann, T.; Tingaut, P. *Environ. Sci. Technol.* **2015**, *49*, 3167.

22. Long, Y. Z.; Zheng, L. F.; Gu, Y. J.; Lin, H.; Xie, X. Y. *Polymer* **2014**, *55*, 6494.

23. Qi, G.; Wang, Y.; Estevez, L.; Duan, X.; Anako, N.; Park, A. A.; Li, W.; Jones, C. W.; Giannelis, E. P. *Energy Environ. Sci.* **2011**, *4*, 444.

24. Wang, J.; Chen, H.; Zhou, H.; Liu, X.; Qiao, W.; Long, D.; Ling, L. *J. Environ. Sci.* **2013**, *25*, 124.

25. Li, P.; Ge, B.; Zhang, S.; Chen, S.; Zhang, Q.; Zhao, Y. *Langmuir* **2008**, *24*, 6567.